Theory of phase-locking in generalized hybrid Josephson-junction arrays

M. Basler,* W. Krech,† and K. Yu. Platov‡
Friedrich-Schiller-Universität Jena, Institut für Festkörperphysik, Max-Wien-Platz 1, D-07743 Jena, Germany
(Received 24 May 1996)

A recently proposed scheme for the analytical treatment of the dynamics of two-dimensional hybrid Josephson-junction arrays is extended to a class of generalized hybrid arrays with ''horizontal'' shunts involving a capacitive as well as an inductive component. This class of arrays is of special interest, because the internal cell coupling has been shown numerically to favor in-phase synchronization for certain parameter values. As a result, we derive limits on the circuit design parameters for realizing this state. In addition, we obtain formulas for the flux-dependent frequency including flux-induced switching processes between the in-phase and antiphase oscillation regime. The treatment covers unloaded arrays as well as arrays shunted via an external load. [S0163-1829(97)00502-X]

I. INTRODUCTION

Two-dimensional (2D) Josephson-junction arrays are considered as strong candidates for tunable microwave oscillators. Since the pioneering works by Benz and Burroughs[1,2] there were some attempts to fabricate arrays of this type[3–5] as well as to understand them theoretically.[6–9] (For two recent reviews on 2D Josephson-junction arrays, see Lachenmann[10] and Booi[11].) While radiation output of two-dimensional arrays should be much larger than that of one-dimensional arrays (for quadratic arrays in the matched case typically $\sim N^2$, with N=number of rows, compared to being $\sim N$, with N=number of junctions, for one-dimensional arrays[6,12]) observations point more to the opposite direction. While in one-dimensional arrays there were observed up to 160 μW,[13,11] the output power reported in two-dimensional arrays is several orders of magnitude smaller with a maximum of around 400 nW.[2,14,15]

Potentially, there can be several reasons responsible for this discrepancy. Besides low critical currents/normal resistances, mismatch to the external load, or parameter tolerances some more basic problems might be responsible for this. Indeed, some recent theoretical investigations show, that the radiating in-phase mode is neutrally stable in an unshunted array without external flux[6] and, even worse, that it is unstable even for a small flux entering the cell.[16] As a result, the natural state of at least the simple model circuit studied in Ref. 16 is a nonradiating one with both cells oscillating against each other. The situation can be improved by adding an appropriate external shunt synchronizing in-phase via its long-range interaction, but generally there remains a tendency that pairs of cells lock antiphase and drop out of the radiating mode.

A recently proposed layout[17] removes this difficulty by introducing an additional capacitive shunt in the ''horizontal'' branches thus turning the internal coupling to favor the in-phase state. It is the aim of the present investigation, to give this idea an analytical foundation and derive some rigorous results, notably on the parameter boundaries separating in-phase from antiphase oscillations. In addition, we study the interplay with an external load leading to a rather complex picture of possible stability regions as a result of the competition of external and internal synchronization.

We start with an exposition of the problem including the basic equations in Sec. II. In Secs. III and IV these equations are solved by an analytical approximation, combining ideas of the strong-coupling method appropriate for small-inductance Josephson-junction cells[18] with the standard weak-coupling procedure of the slowly varying phase[19–21] for the treatment of intercell coupling. While Sec. III contains lowest-order results corresponding to vanishing cell inductance, Sec. IV includes the effects caused by a small, but nonvanishing inductance being essential for understanding the intercell coupling. Section V contains several results including a comparison with numerical simulations. The interplay with an external load is treated in Sec. VI, and Sec. VII contains several more general conclusions relevant for the layout of two-dimensional Josephson-junction arrays.

II. THE MODEL AND THE BASIC EQUATIONS

For making the problem accessible to an analytical treatment, we have to make several propositions. Figure 1 shows the circuit under consideration. To make the physical mechanisms more transparent, the external shunt Z_L is removed in the beginning, and will only be included in Sec. VI. Despite its simplicity this model has all the main features present in

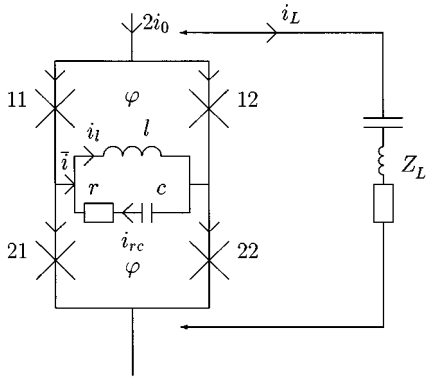

FIG. 1. The generalized Josephson-junction hybrid array model circuit under investigation.

larger arrays, too: It is truly two-dimensional with a possible flux entering the cells. Notice, that unlike conventional hybrid arrays[5,8] the horizontal branch contains a more general shunt consisting not only of the usual inductive connection, but of a parallel capacitance and resistance. Numerical results obtained before indicate that an intrinsic shunt of this type can favor in-phase locking even in an externally unshunted array. Here, we will confirm and extend this result by developing an analytical formalism which should be applicable to larger two-dimensional arrays with the same general structure as well.

Some more restrictions have to be put on the array: (i) Josephson junctions are described by the resistively shunted junction (RSJ) model.[12] (ii) All junctions are considered to be identical. (iii) Junctions are overdamped with a McCumber parameter set to zero. (iv) Self-inductance is taken into account while mutual inductance is neglected. (v) The normalized ring inductance between the two loops

$$l=2\pi I_C L/\Phi_0 \tag{1}$$

is supposed to be small ($l\ll 1$). From the beginning, one has to understand that the inductance of the horizontal connection acts in a twofold way. At first, it contributes to both ring inductances thus determining the superconducting quantum interference device (SQUID) coupling within each loop. At second, it is part of the shunt common to both loops and as such it influences the intercell coupling. With Eq. (1) we request the SQUID coupling to be strong, which is a necessary prerequisite for our approximation scheme to work. On the other hand, we will not fix the ratio between the inductive and the capacitive horizontal impedances from the beginning.

In the following, we will exploit some more normalized quantities as follows,

$$s=\frac{2e}{\hbar}I_C R_N t, \tag{2}$$

$$\varphi=2\pi\Phi/\Phi_0, \tag{3}$$

$$c=\frac{2e}{\hbar}I_C R_N^2 C, \tag{4}$$

$$r=R/R_N, \tag{5}$$

$$i=I/I_C, \tag{6}$$

with I_C the junction critical current, R_N is the normal resistance of one of the (identical) junctions, Φ is the external flux per cell, and the last normalization being valid for all currents entering the calculation. Adopting these normalizations, the circuit can be described by the RSJ equations for the Josephson phases,

$$\dot{\phi}_{ij}+\sin\phi_{ij}=i_{ij}, \quad (\{i,j\}=\{1,2\}) \tag{7}$$

in conjunction with the two flux quantization conditions

$$\phi_{i2}-\phi_{i1}-\varphi\mp l i_l=0 \tag{8}$$

(minus sign refers to $i=1$) and Kirchhoff's current laws

$$i_0=\frac{1}{2}(i_{11}+i_{12}), \tag{9}$$

$$\overline{i}=i_{11}-i_{21}=i_{22}-i_{12}, \tag{10}$$

$$i_l=\overline{i}+i_{rc}. \tag{11}$$

These have to be supplemented by Kirchhoff's voltage law

$$\ddot{i}_l+\frac{r}{l}\dot{i}_{rc}+\frac{1}{lc}i_{rc}=0. \tag{12}$$

We would like to point out that while the inductive branch carrying current i_l is part of both superconducting loops thus contributing to the flux quantization conditions (8), the branch i_{rc} enters only via the ordinary Kirchhoff's law (12). As a result, it is impossible to simply substitute the three elements l, c, and r by a single impedance Z from the beginning.

Before, it has proven useful in the treatment of strongly coupled SQUID cells[18] to combine the Josephson phases within each cell via

$$\Sigma_k=\frac{1}{2}(\phi_{k2}+\phi_{k1}), \tag{13}$$

$$\Delta_k=\frac{1}{2}(\phi_{k2}-\phi_{k1}). \tag{14}$$

In addition, we introduce the circular currents

$$i_k^\circ=(i_{k2}-i_{k1})/2. \tag{15}$$

With the help of Eqs. (13)–(15) we finally obtain the system

$$\dot{\Sigma}_k+\sin\Sigma_k\cos\Delta_k=i_0, \tag{16a}$$

$$\dot{\Delta}_k+\sin\Delta_k\cos\Sigma_k=i_k^\circ, \tag{16b}$$

$$\Delta_1+\Delta_2-\varphi=0, \tag{16c}$$

$$\Delta_1-\Delta_2=l i_l=l(i_2^\circ-i_1^\circ+i_{rc}), \tag{16d}$$

$$\ddot{i}_{rc}+\frac{r}{l}\dot{i}_{rc}+\frac{1}{lc}i_{rc}=(\ddot{i}_1^\circ-\ddot{i}_2^\circ) \tag{16e}$$

which our analytical approximation scheme is based on. As there are seven equations for the seven variables $\Sigma_k,\Delta_k,i_k^\circ,i_{rc}$, this is a well-posed problem.

III. ANALYTICAL APPROXIMATION SCHEME AND LOWEST-ORDER RESULTS

Our strategy for solving system (16) will be based on a perturbative treatment valid for small l (for the basic idea compare our earlier paper[18]). Thus, we start solving Eqs. (16) for $l=0$, and only later include corrections $\sim l$ exploiting the lowest-order results obtained before. This procedure is favored by the fact that l enters Eq. (16d) only. We start by evaluating Eq. (16d) in conjunction with Eq. (16c). The solutions for Δ_k can be used to evaluate Σ_k from Eq. (16a). Next, we find the i_k° (not the Δ_k, which are already known in

this order) from Eq. (16b). Finally, with the ring currents i_k° on the right-hand side of Eq. (16e) known we can evaluate the current i_{rc} by solving the corresponding differential equation. All other quantities, like i_l or i, are secondary and can be derived from the seven variables mentioned so far. Afterwards, we insert the lowest-order result on the right-hand side of Eq. (16d) and start a second cycle in the same sequence.

The procedure described above gives the following lowest-order results. First, the Josephson phase differences in both loops are found to be identical,

$$\Delta_{k,0}=\varphi/2. \tag{17}$$

In the following, comma-delimited indices refer to the order of approximation. From Eq. (16a), the Josephson phases are found to coincide with the corresponding solutions for an autonomous junction,[12]

$$\Sigma_{k,0}=\frac{\pi}{2}+2\arctan\left(\frac{\zeta_0}{i_0+\cos(\varphi/2)}\tan\frac{\zeta_0 s-\delta_k}{2}\right), \tag{18}$$

with the important modification that the frequency ζ_0 becomes flux dependent according to

$$\zeta_0=\sqrt{i_0^2-\cos^2(\varphi/2)}. \tag{19}$$

Next, the circular currents can be evaluated from Eq. (16b). Note, that this equation originating from the original Josephson equations does not lead to a differential equation, because the constant Josephson phase differences Δ_k are already known. The result is

$$i_k^\circ=\sin(\varphi/2)\cos\Sigma_{k,0}. \tag{20}$$

It is a trivial task to evaluate Eq. (20) using Eq. (18); in the further calculation we will only need the lowest harmonics of the circular currents,

$$i_{k,0}^\circ=-2\frac{\zeta_0}{i_0+\zeta_0}\sin(\varphi/2)\sin(\zeta_0 s-\delta_k). \tag{21}$$

The corresponding difference of the ring currents,

$$\overline{i}_{,0}=i_{2,0}^\circ-i_{1,0}^\circ=4\frac{\zeta_0}{i_0+\zeta_0}\sin(\varphi/2)\sin\left(\frac{\delta_1-\delta_2}{2}\right)\times\cos\left(\zeta_0 s-\frac{\delta_1+\delta_2}{2}\right), \tag{22}$$

enters the horizontal connection thus acting as a driving force for the oscillatory circuit according to Eq. (16e). This equation can be solved with standard methods. The stationary oscillating solution reads

$$i_{rc,0}=-\frac{4l\zeta_0^2}{|Z(\zeta_0)|(i_0+\zeta_0)}\sin(\varphi/2)\sin\left(\frac{\delta_1-\delta_2}{2}\right)\times\sin\left(\zeta_0 s-\frac{\delta_1+\delta_2}{2}-\psi(\zeta_0)\right). \tag{23}$$

Here, we introduced the series circuit impedance Z with

$$|Z(\zeta_0)|=\sqrt{r^2+\left(\frac{1}{c\zeta_0}-l\zeta_0\right)^2} \tag{24}$$

and the phase angle ψ,

$$\cos\psi(\zeta_0)=\frac{r}{|Z(\zeta_0)|},\quad \sin\psi(\zeta_0)=\frac{l\zeta_0-1/c\zeta_0}{|Z(\zeta_0)|}. \tag{25}$$

For later purposes we need $i_l=\overline{i}+i_{rc}$ rather than i_{rc}, because it is just i_l which potentially may split the oscillation phases between cell 1 and cell 2 via Eq. (16d). Combining Eq. (23) with Eq. (22) after some algebra we obtain

$$i_{l,0}=-\frac{4\zeta_0}{i_0+\zeta_0}\frac{|z(\zeta_0)|}{|Z(\zeta_0)|}\sin(\varphi/2)\sin\frac{\delta_1-\delta_2}{2}\times\cos\left(\zeta_0 s-\frac{\delta_1+\delta_2}{2}-\chi(\zeta_0)\right), \tag{26}$$

where we introduced the rc impedance $|z|$ with

$$|z(\zeta_0)|=\sqrt{r^2+\frac{1}{(c\zeta_0)^2}} \tag{27}$$

and

$$\sin\chi(\zeta_0)=\frac{rlc\zeta_0^2}{|Z(\zeta_0)|\sqrt{1+(rc\zeta_0)^2}},\qquad \cos\chi(\zeta_0)=\frac{r^2c\zeta_0+(1/c\zeta_0-l\zeta_0)}{|Z(\zeta_0)|\sqrt{1+(rc\zeta_0)^2}}. \tag{28}$$

[In principle, one could evaluate i_l directly from an equation similar to Eq. (16e) of course, and we checked that the result is the same. The procedure described here has the advantage of additionally providing an expression for the current flowing through the capacitive line.]

To summarize, we observe the following lowest-order results: All four junctions oscillate with the same flux-dependent frequency $\zeta_0=\sqrt{i_0^2-\cos^2(\varphi/2)}$. Because of Eq. (17), the junctions within each cell are exactly in phase, while the relative phase between cell 1 and cell 2 (given by δ_1 and δ_2, respectively) is undetermined, up to now. If both cells are in phase, there is no current through the horizontal line, because of the $\sin[(\delta_1-\delta_2)/2]$ present in Eq. (22). On the other hand, the horizontal current reaches its maximum if both cells oscillate antiphase with $\delta_1-\delta_2=\pi$.

IV. INDUCTANCE EFFECTS

Now we are ready to include inductance effects. Again starting with Eqs. (16c) and (16d), we insert the lowest-order result Eq. (26) on the right-hand side of Eq. (16d). This leads to

$$\Delta_{1/2}=\Delta_{1/2,0}+l\Delta_{1/2,1}=\frac{\varphi}{2}\pm 2l\frac{\zeta_0}{i_0+\zeta_0}\frac{|z|}{|Z|}\sin(\varphi/2)\sin\frac{\delta_2-\delta_1}{2}$$
$$\times\cos\left(\zeta_0 s-\frac{\delta_1+\delta_2}{2}-\chi\right). \tag{29}$$

Note, that the first index in Eq. (29) refers to cell 1 and cell 2, respectively, while the second one indicates the order of evaluation; the + sign refers to Δ_1. This has to be inserted into Eq. (16a),

$$\dot{\Sigma}_k+\cos(\Delta_{k,0}+l\Delta_{k,1})\sin\Sigma_k=i_0. \tag{30}$$

For evaluating these equations the cosine on the left-hand side is expanded according to

$$\cos(\Delta_{k,0}+l\Delta_{k,1})\approx\cos\Delta_{k,0}-l\Delta_{k,1}\sin\Delta_{k,0}. \tag{31}$$

After transferring the correction term $\sim l$ to the right-hand side of Eq. (30) one makes the crucial observation, that it acts in a similar way as, for example, an external shunt synchronizing the cells.[19]

The resulting equations are evaluated with the conventional phase-slip method (see, for instance, Refs. 19–21). According to this procedure which has proven useful in the treatment of linear arrays before, the up to now constant phases δ_1 and δ_2 are considered as time dependent,

$$\delta_k=\delta_k(s), \tag{32}$$

with the subsidiary condition that this time dependence is only an adiabatic one,

$$\dot{\delta}\ll\zeta_0. \tag{33}$$

Physically, this means that the phases are required to be nearly constant during one Josephson oscillation.

With these assumptions, the same ansatz (18) with $\delta_k(s)$ and ζ instead of ζ_0 leads to the sum voltages $\dot{\Sigma}_k$,

$$\dot{\Sigma}_k=\frac{\zeta_0(\zeta-\dot{\delta}_k)}{i_0+\cos(\varphi/2)\cos(\zeta s-\delta_k)}. \tag{34}$$

Writing ζ instead of ζ_0 we have allowed for a possible (small) deviation of the actual oscillation frequency from ζ_0. Inserting Eq. (34) into (30) leads to the reduced equations

$$\zeta_0(\zeta-\zeta_0-\dot{\delta}_k)=l\ \sin(\varphi/2)\Delta_{k,1}[\cos(\varphi/2)+i_0\cos(\zeta s-\delta_k)]. \tag{35}$$

After averaging over one time period and applying some algebra we arrive at the following system of equations (for details see, for instance, Refs. 16 and 19–21)

$$\zeta_0(\zeta-\zeta_0-\langle\dot{\delta}_1\rangle)=li_0\frac{\zeta_0}{i_0+\zeta_0}\frac{|z|}{|Z|}\sin(\varphi/2)\sin\frac{\langle\delta_2\rangle-\langle\delta_1\rangle}{2}$$
$$\times\sin(\varphi/2)\cos\left(\frac{\langle\delta_2\rangle-\langle\delta_1\rangle}{2}+\chi\right), \tag{36a}$$

$$\zeta_0(\zeta-\zeta_0-\langle\dot{\delta}_2\rangle)=-li_0\frac{\zeta_0}{i_0+\zeta_0}\frac{|z|}{|Z|}\sin(\varphi/2)\sin\frac{\langle\delta_2\rangle-\langle\delta_1\rangle}{2}$$
$$\times\sin(\varphi/2)\cos\left(\frac{\langle\delta_2\rangle-\langle\delta_1\rangle}{2}+\chi\right), \tag{36b}$$

where $\langle\ \rangle$ denotes the time average over one Josephson oscillation. The difference of Eqs. (36a) and (36b) gives an evolution equation for the phase difference $\langle\delta\rangle$,

$$\langle\dot{\delta}\rangle=\frac{i_0 l}{i_0+\zeta_0}\frac{|z|}{|Z|}\sin^2(\varphi/2)\cos\chi\sin\langle\delta\rangle. \tag{37}$$

Equation (37) is the basic equation determining the possible phase differences between the oscillations of both cells as well as the corresponding regions of stability.

V. PHASE-LOCKING, STABILITY AND OSCILLATION FREQUENCY

We will not go into the question of general solutions of Eq. (37) but concentrate on phase-locking, being characterized by a time-independent phase shift between cell 1 and cell 2,

$$\langle\dot{\delta}^{\text{lock}}\rangle=0. \tag{38}$$

Within the range $0\leqslant\delta<2\pi$ there are obviously only two possibilities for Eq. (38) to be valid,

$$\langle\delta^{\text{lock}}\rangle=0\quad\text{and}\quad\langle\delta^{\text{lock}}\rangle=\pi, \tag{39}$$

the first one describing in-phase oscillations and the second one antiphase oscillations of the cells.

The crucial question of the range of stability of these two solutions can be answered on the basis of the evolution equation (37), too. The ansatz

$$\langle\delta\rangle=\langle\delta^{\text{lock}}\rangle+ae^{\lambda t} \tag{40}$$

($|a|\ll|1|$) leads to the Lyapunov coefficient

$$\lambda=\frac{i_0 l}{i_0+\zeta_0}\frac{|z|}{|Z|}\sin^2(\varphi/2)\cos\chi\cos\langle\delta^{\text{lock}}\rangle. \tag{41}$$

One recovers that the stability is solely determined by the $\cos\chi$; all the remaining factors, except δ^{lock}, are positive definite. In detail, the

$$\text{in-phase solution}\ \langle\delta^{\text{lock}}\rangle=0\ \text{is stable for}\ \cos\chi<0, \tag{42}$$

while the

$$\text{antiphase solution}\ \langle\delta^{\text{lock}}\rangle=\pi\ \text{is stable for}\ \cos\chi>0. \tag{43}$$

Before further evaluating this condition we will consider the oscillation frequency which can be derived from Eq. (36a) [or Eq. (36b)]. With

$$\langle\delta_1\rangle=\langle\delta_2\rangle=\text{const}=0, \tag{44}$$

one easily recovers

$$\zeta^{\text{in}}=\zeta_0=\sqrt{i_0^2-\cos^2(\varphi/2)}. \tag{45}$$

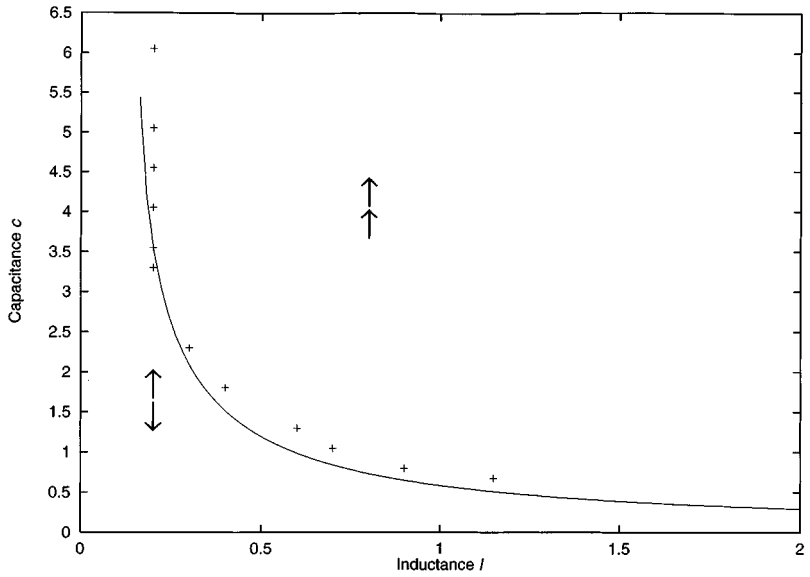

FIG. 2. The boundary between in-phase and antiphase oscillations. Solid line: analytical approximation. Crosses: numerical simulation. Parameters: $i_0=1.5, r=0.1, \varphi=1.0$.

Evaluating the antiphase frequency with

$$\langle \delta_1 \rangle - \langle \delta_2 \rangle = \pi \tag{46}$$

needs a bit more algebra. The result is

$$\zeta^{\text{anti}} = \zeta_0 \left(1 - \frac{i_0 l^2 r \sin^2(\varphi/2)}{|Z|^2 (i_0 + \zeta_0)} \right). \tag{47}$$

Thus, if both cells oscillate in-phase their frequency is identical to the autonomous oscillation frequency. On the other hand, if the cells oscillate antiphase the frequency will be lower than ζ_0. The physical reason for this behavior can be understood by comparing with other (even linearly) oscillating systems: If the bindings (in our case realized by the horizontal impedance) are not loaded, the oscillation frequency remains the same as for uncoupled oscillators; if the bindings are loaded (i.e., in case of an ac current flowing through the horizontal line) the system oscillates with a different frequency.

Unfortunately, one has to respect a certain limit of validity of Eq. (47). Using the method of slowly varying phase we have adopted the supposition mentioned before that the frequency must not deviate too much from ζ_0,

$$\zeta \approx \zeta_0 . \tag{48}$$

Thus, the correction in Eq. (47) is required to be small compared to the frequency itself. A rough estimate valid for $i_0 > 1.15$ leads to the condition

$$l^2 \ll r. \tag{49}$$

Our experience shows that usually a factor of $2 \ldots 3$ is sufficient for this condition to be fulfilled.

Now we return to the question of antiphase$\leftrightarrow$in-phase transitions described by Eqs. (42) and (43), respectively. Considering the numerator of $\cos\chi$ one observes that the boundary separating in-phase and antiphase oscillations of the cells is given by

$$\left(\frac{1}{c\zeta} - l\zeta \right) + r^2 c \zeta = 0 \tag{50}$$

with the cells oscillating anti-phase if the left hand side is positive and in-phase if it is negative. In other words, the transition between both regimes lies in the vicinity of the resonance curve of the l-c-r connection with deviations becoming important for small l. Figure 2 shows the boundary between the two regimes for a frequency $\zeta = 1.11$ in comparison to numerical results.

To summarize, the in-phase regime is favored for not too large r as long as the inductive impedance dominates over the capacitive one, while for the capacitive impedance dominating the cells oscillate antiphase. There is a simple physical explanation for this: Anti-phase oscillations are caused by the flux coupling via the joint inductive line carrying current i_l. For a sufficiently large capacitive shunt, the current prefers the capacitive way which does not produce any such flux.

In conventional hybrid arrays[8] horizontal lines are purely inductive. Formally, this limit can be observed letting $c \to 0$. In this case the capacitive impedance goes to infinity while the correction $\sim r^2 c$ tends to zero. Then, there is no possibility for the current to be shunted, and the cells remain in the antiphase regime.[16] The more general question, for which parameter values l, c, and r there are no transitions can be answered on the basis of Eq. (50). This equation does only have real solutions for ζ if

$$l > r^2 c. \tag{51}$$

For all smaller l, the current in the inductive line is strong enough to keep the cells oscillating antiphase.

Considering the circuit parameters i_0, l, etc. as constant and leaving the external flux φ as the only free parameter one can observe flux-induced transitions between both regimes. The difference between the frequencies ζ^{in} and ζ^{anti} leads to a hysteresis, which has been observed in numerical simulations before.[17] In more detail, in-phase$\to$antiphase transitions are observed at

$$\varphi^{\text{ia}} = 2 \arccos[\pm \sqrt{i_0^2 - \zeta^{\text{tr2}}}], \tag{52}$$

where we introduced the transition frequency

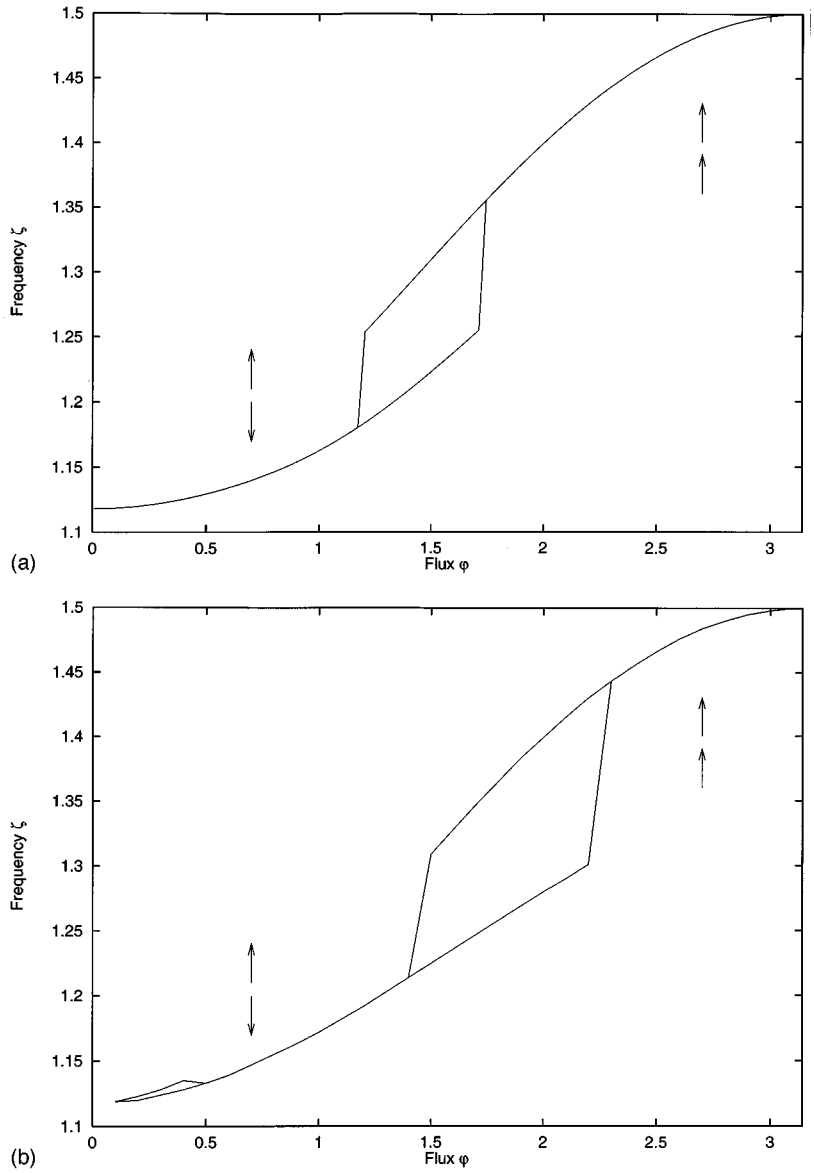

FIG. 3. Frequency against flux with a transition from antiphase to in-phase oscillations. Parameters: $i_0=1.5, r=0.1, l=0.2, c=4.0$. (a) Analytical approximation. (b) Numerical simulation.

$$\zeta^{\mathrm{tr}}=\frac{1}{\sqrt{lc-r^2c^2}} \tag{53}$$

as can be easily deduced from Eq. (50). The transition from the antiphase to the in-phase regime needs a bit more algebra. It can be determined from the requirement, that the antiphase frequency Eq. (47) be equal to the transition frequency Eq. (53). Unfortunately, the resulting equation cannot be solved in closed form. However, as a first approximation, one can equate the in→antitransition frequency (53) with Eq. (47) and evaluate for φ, substituting $\zeta\rightarrow\zeta^{\mathrm{tr}}$ on the right-hand side of Eq. (47),

$$\varphi^{\mathrm{ai}}=2\arccos\left(\pm\sqrt{\frac{i_0^2-(\zeta^{\mathrm{tr}})^2-2i_0l/cr(i_0+\zeta^{\mathrm{tr}})}{1-2i_0l/cr(i_0+\zeta^{\mathrm{tr}})}}\right). \tag{54}$$

It can be deduced, that φ^{ai} is always larger than φ^{ia}. A better result for φ^{ai} is obtained by graphically finding the transition frequency on the curve at $\zeta=\zeta^{\mathrm{tr}}$.

Thus, if there are any transitions between both regimes at all, for small values of the external flux the cells oscillate with the lower antiphase frequency switching to in-phase oscillations at φ^{ai}. Because of $\varphi^{\mathrm{ai}}>\varphi^{\mathrm{ia}}$ (for $0<\varphi\leqslant\pi$) switching back to the antiphase state occurs at a lower flux, leading to the hysteresis mentioned above. Figure 3 shows a plot of frequency against flux in comparison with the outcome of a numerical simulation. The frequencies are in excellent agreement, and even the transition points, which depend rather sensibly on the parameters, are located within the same region.

This last result concerning hysteresis has to be taken with some care. It was obtained by combining the antiphase frequency formula (47) with Eq. (50) and evaluating for φ. However, Eq. (50) as originating from Eq. (37) is already a first-order result, thus inserting Eq. (47) might not be fully justified, while second-order terms in (37) are neglected. Nonetheless, it gives a plausible explanation for the mechanism causing the hysteresis observed in numerical simulations.

VI. LONG-RANGE SYNCHRONIZATION VIA AN EXTERNAL LOAD

It has been well-known for a long time that synchronization in a one-dimensional array can be achieved and controlled by shunting the array via an external load.[19,22] In a similar manner one may hope to be able to control row locking in two-dimensional arrays, too. For studying this mechanism within our model we now add the external load already indicated in Fig. 1. As a result, we have to supplement the basic equations (16). At first, we add the mesh rule for the load current i_L,

$$\sum_{k=1,2} \ddot{\Sigma}_k - l_L \ddot{i}_L - r_L \dot{i}_l - \frac{1}{c_L} i_L = 0. \tag{55}$$

Here, r_L, l_L, and c_L are the load impedances normalized in the same manner as Eqs. (1), (4), and (5). In addition, the load current couples back to the junctions, thus supplementing Eq. (16a),

$$\dot{\Sigma}_k + \sin\Sigma_k \cos\Delta_k = i_0 - \frac{1}{2} i_L . \tag{56}$$

As has been observed in the study of similar one-dimensional synchronization problems before, the reciprocal impedance $1/|Z_L| \ll 1$ provides another perturbation parameter for a sufficiently large load; thus we evaluate the system perturbatively, neglecting terms $\sim l/|Z_L|$. To lowest order with respect to $|Z_L|$ the load current vanishes, and we end up with the results described in Sec. III. Based on the lowest-order Josephson oscillations (18) and the corresponding voltages $\dot{\Sigma}_{k,0}$ we obtain the first-order (with respect to $1/|Z_L|$) load current $i_{L,0}$,

$$i_{L,0} = \frac{4\cos(\varphi/2)}{|Z_L|} \frac{\zeta_0}{i_0+\zeta_0} \cos\left(\frac{\delta_1-\delta_2}{2}\right) \sin\left(\zeta_0 s - \frac{\delta_1+\delta_2}{2} - \psi_L\right) \tag{57}$$

with

$$|Z_L(\zeta_0)| = \sqrt{(r_L+1)^2 + \left(\frac{1}{c_L\zeta_0} - l_L\zeta_0\right)^2}, \tag{58a}$$

$$\sin\psi_L(\zeta_0) = \frac{r_L+1}{|Z_L(\zeta_0)|}, \tag{58b}$$

$$\cos\psi_L(\zeta_0) = \frac{1/c_L\zeta_0 - l_L\zeta_0}{|Z_L(\zeta_0)|}. \tag{58c}$$

Its structure is obviously quite similar to that of the horizontal current Eq. (22). However, one should note two differences: (i) While the load current is maximal for $\varphi = 0$, the horizontal current reaches its maximum for $\varphi = \pi/2$. (ii) The horizontal current vanishes if both cells oscillate in-phase, while the load current vanishes for both cells oscillating antiphase.

The load current Eq. (57) provides the additional contribution to Eq. (56) and, as a result, the phase-slip equations (36) get an additional term, too. After performing the time averages we get

$$\begin{aligned}\zeta_0(\zeta - \zeta_0 - \langle\dot{\delta}_1\rangle) = &-\frac{i_0 l}{2} \frac{\zeta_0}{i_0+\zeta_0} \frac{|z|}{|Z|} \sin^2(\varphi/2) \\ &\times[\sin\psi + \sin(\langle\delta_1\rangle - \langle\delta_2\rangle - \chi)] \\ &+ \frac{1}{2} \frac{\zeta_0}{i_0+\zeta_0} \frac{1}{|Z_L|} \cos^2(\varphi/2) \\ &\times[\sin\psi_L - \sin(\langle\delta_1\rangle - \langle\delta_2\rangle - \psi_L)],\end{aligned} \tag{59a}$$

$$\begin{aligned}\zeta_0(\zeta - \zeta_0 - \langle\dot{\delta}_2\rangle) = &\frac{i_0 l}{2} \frac{\zeta_0}{i_0+\zeta_0} \frac{|z|}{|Z|} \sin^2(\varphi/2)[\sin\psi + \sin(\langle\delta_1\rangle \\ &- \langle\delta_2\rangle - \chi)] + \frac{1}{2} \frac{\zeta_0}{i_0+\zeta_0} \frac{1}{|Z_L|} \cos^2(\varphi/2) \\ &\times[\sin\psi_L + \sin(\langle\delta_1\rangle - \langle\delta_2\rangle - \psi_L)].\end{aligned} \tag{59b}$$

By subtracting Eqs. (59a) and (59b), we finally get the evolution equation for the averaged oscillation phase difference,

$$\begin{aligned}\langle\dot{\delta}\rangle = \frac{1}{i_0+\zeta_0} \Bigg(&\frac{1}{|Z_L|} \cos^2(\varphi/2)\cos\psi_L \\ &+ i_0 l \frac{|z|}{|Z|} \sin^2(\varphi/2)\cos\chi \Bigg) \sin\langle\delta\rangle.\end{aligned} \tag{60}$$

Despite the relatively complicated interplay between cell interaction via the horizontal line and long-range coupling via the external load there remain only the same two phase-locking solutions as before,

$$\langle\delta^{\text{lock}}\rangle = 0 \quad \text{and} \quad \langle\delta^{\text{lock}}\rangle = \pi, \tag{61}$$

the stability of which is determined by the Lyapunov coefficient

$$\begin{aligned}\lambda = \frac{1}{i_0+\zeta_0} \Bigg(&\frac{1}{|Z_L|} \cos^2(\varphi/2)\cos\psi_L + i_0 l \frac{|z|}{|Z|} \sin^2(\varphi/2)\cos\chi \Bigg) \\ &\times \cos\langle\delta^{\text{lock}}\rangle.\end{aligned} \tag{62}$$

In-phase oscillations of the cells are stable if the term in parentheses is lower than zero, while antiphase oscillation are stable if it is greater than zero. Thus, the desired stability for the in-phase mode is reached for

$$\frac{1}{|Z_L|} \cos^2(\varphi/2)\cos\psi_L + i_0 l \frac{|z|}{|Z|} \sin^2(\varphi/2)\cos\chi < 0. \tag{63}$$

Equation (63) shows a rather complex parameter dependence, relating the seven parameters r, l, c, r_L, l_L, c_L, and φ. Its physical meaning is best discovered considering several limiting cases.

(i) For a sufficiently large external load,

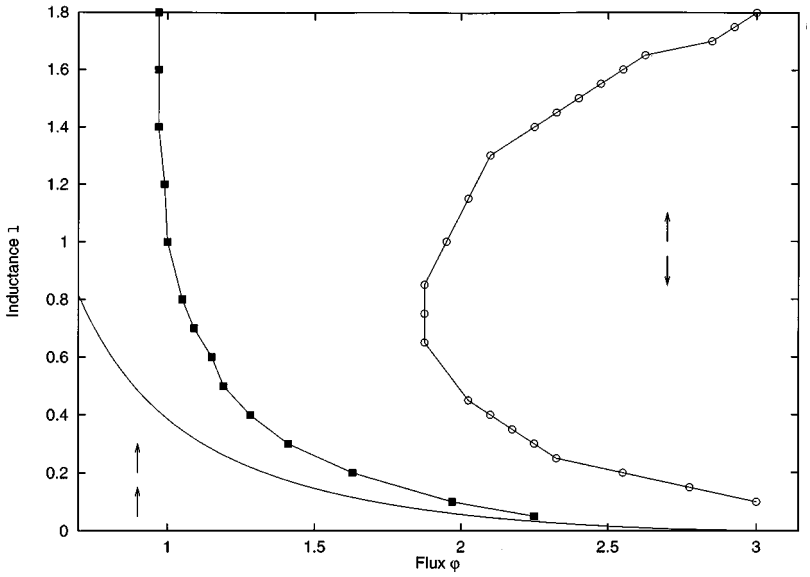

FIG. 4. Transition between in-phase and antiphase state caused by the internal inductive coupling present in a hybrid array. Parameters: $i_0=1.5, r_L=1.0, l_L=1.0, c_L=2.0$. Solid line: analytical approximation, boxes: numerical simulation, open dots: numerical simulation with inductance regularly distributed around loops.

$$\frac{1}{|Z_L|} \ll i_0 l \frac{|z|}{|Z|}, \tag{64}$$

the relative phase of the cells is determined by the internal coupling alone. This has to be compared to the case of two externally loaded separate cells.[23] In this case—as for linear arrays—the relative phase depends on the character of the external load only: While for inductively dominated loads the cells are locked in-phase, they are locked antiphase for capacitively dominated loads, independently of the magnitude of the external load.

(ii) The contributions from the external load and from the internal shunt show a different flux dependence. For sufficiently small values of external flux the last term can be neglected, and the locking regime is controlled by the load only. On the other hand, for flux values of around half a flux quantum the first term becomes negligible, and the internal horizontal line determines the phase difference of the cells.

(iii) For $l \to 0$, the second term can be neglected, and the result agrees with that obtained for two separate cells before,[23] as it should be. In this limit the cells internally decouple, while the external coupling remains in force.

(iv) The usual hybrid arrays without the internal R-C line are contained as a limiting case. For $r \to \infty$, the in-phase condition, Eq. (63), reduces to

$$\frac{1}{|Z_L|} \cos\psi_L \cos^2(\varphi/2) + i_0 l \sin^2(\varphi/2) < 0. \tag{65}$$

It states, that for sufficiently large inductances,

$$l > l^{\mathrm{cr}} = -\frac{\cos\psi_L}{i_0 \tan^2(\varphi/2)|Z_L|}, \tag{66}$$

ordinary pure inductive hybrid arrays may switch to the antiphase state even for inductive external loads.

The indicated transition was indeed observed in a numerical simulation (boxes in Fig. 4). Having in mind that Eq. (65) is the result of several approximations, concerning the external shunt as well as the internal inductive coupling, the agreement is remarkably good.

The influence of changing parameters can be nicely illustrated by performing a second simulation with exactly the same parameter set, but distributing ring inductance l regularly around the loops. The result denoted by the dots in Fig. 4 clearly deviates from that obtained for inductance concentrated on the horizontal line considered before. This can be taken as a strong indication that the coupling is not provided by the loop inductances but by the inductance on the line common to both cells.

VII. CONCLUSIONS

Although our work is devoted to the study of a simple model circuit several results are expected to be valid for larger arrays, too. At first, the short-range coupling between neighboring cells leads to an antiphase synchronization in conventional Josephson-junction hybrid arrays. This may be one reason for explaining the very small radiation output in 2D Josephson-junction arrays obtained so far. Second, we show a way to improve the situation by adding a capacitive shunt parallel to the horizontal lines. In this way, the flux-generating current potentially responsible for the antiphase coupling is redirected through the capacitive line which is not part of a flux quantization condition.

Combining Fig. 2 with some already known facts on synchronization in strongly coupled SQUID cells[18] the following design criteria for generalized hybrid 2D Josephson-junction arrays can be derived. (i) For synchronizing horizontal lines in-phase the ring inductances have to be kept small ($l \ll 1$). (ii) In-phase synchronization between neighboring cells in vertical direction is observed for $l > 1/c\zeta^2 + r^2 c$. Based on this, we will derive some estimates for reasonable c and l. For a given l, the boundary between in- and antiphase oscillations is given by Eq. (50). Figure 2 shows already that the additional term $\sim r$ restricts the possible l by setting a lower bound. This bound is obtained from

$$\frac{\mathrm{d}l}{\mathrm{d}c} = 0 \tag{67}$$

as

$$r=\frac{1}{c\zeta} \quad \text{resp.} \quad l=2r/\zeta. \tag{68}$$

Thus, for obtaining in-phase oscillations the condition

$$r<\frac{\zeta l}{2} \tag{69}$$

has to be respected. Because of Eq. (68) this means

$$c>\frac{2}{l\zeta}. \tag{70}$$

Obviously, the requirement to have a small l for horizontal in-phase synchronization leads to the demand to have a sufficiently high capacitance $c>2/l\zeta$ as well as a small resistance $r<l\zeta/2$. A reasonable compromise might, for instance, be

$$l\approx 0.8, \quad c\approx 3.0, \quad r\approx 0.2. \tag{71}$$

Of course, all these estimates should be considered as very rough, and on the other hand, one has to check carefully how large these quantities on chip actually are.

On the other hand, we would like to point out that these suggestions are based on an analytical approximation scheme and are founded on solid formulas. Of course, it still has to be shown rigorously that they can be transferred to larger arrays as well. Some preliminary results from numerical simulations indeed indicate this. We hope that the general procedure described here can be transferred to larger arrays of the type considered here as well, and some work is on the way to actually extend it to a ladder configuration.

If the arrays are externally loaded, which is usually done via an inductive load, the parameters have to be chosen in such a manner to respect Eq. (63). The best way for obtaining in-phase synchronization is to make both contributions to the Lyapunov-coefficient lower than zero separately, which is possible because the parameters of the external load can be chosen independently of those from the internal shunt. In general, one should select values such, that (i) the external load is dominated by its inductive contribution, (ii) the internal horizontal shunts are dominated by the inductive impedance, too. Because of the frequency dependence of the characters of the shunts, one has to make sure that these conditions are met for all values of external flux.

Of course, the circuit studied here has several features requiring a more detailed investigation, either analytically or numerically. Usually one exploits shunted tunnel junctions for building arrays, thus one may ask for the influence of nonvanishing McCumber parameters. On the other hand, the influence of parameter splitting needs to be investigated, and in addition, in real arrays, noise comes into play. While this last aspect is to be expected to play only a minor role within the small inductance loops, it will be sure to have some influence on the coupling between the cells.

ACKNOWLEDGMENTS

This work was supported by a project of the Deutsche Forschungsgemeinschaft DFG under Contract No. Kr1172/4-1. The authors would like to express their thanks to the DFG for financial support.

*Electronic address: pmb@rz.uni-jena.de
†Electronic address: owk@rz.uni-jena.de
‡Electronic address: okp@rz.uni-jena.de

[1] S. P. Benz and C. J. Burroughs, Supercond. Sci. Technol. **4**, 561 (1991).
[2] S. P. Benz and C. J. Burroughs, Appl. Phys. Lett. **58**, 2162 (1991).
[3] P. A. A. Booi *et al.*, IEEE Trans. Appl. Supercond. **3**, 2493 (1993).
[4] L. L. Sohn *et al.*, Phys. Rev. B **47**, 975 (1993).
[5] H. Shea, M. Itzler, and M. Tinkham, Phys. Rev. B **51**, 12 690 (1995).
[6] K. Wiesenfeld, S. Benz, and P. Booi, J. Appl. Phys. **76**, 3835 (1994).
[7] G. Filatrella and K. Wiesenfeld, J. Appl. Phys. **78**, 1878 (1995).
[8] R. L. Kautz, IEEE Trans. Appl. Supercond. **5**, 2702 (1995).
[9] M. Darula, P. Seidel, F. Busse, and S. Benacka, J. Appl. Phys. **74**, 2674 (1993).
[10] S. Lachenmann, Ph.D. thesis, Eberhard-Karls-Universität Tübingen, 1995.
[11] P. A. Booi, Ph.D. thesis, Twente University, 1995.
[12] K. K. Likharev, *Dynamics of Josephson Junctions and Circuits* (Gordon and Breach, Philadelphia, 1991).
[13] J. E. Lukens, in *Superconducting Devices*, edited by S. T. Ruggiero and D. A. Rudman (Academic, New York, 1990), pp. 135–167.
[14] J. A. Stern, H. G. LeDuc, and J. Zmudzinas, Trans. Appl. Supercond. **3**, 2485 (1993).
[15] M. Octavio, C. B. Whan, and C. J. Lobb, Appl. Phys. Lett. **60**, 766 (1992).
[16] M. Basler, W. Krech, and K. Platov, J. Appl. Phys. **80**, 3598 (1996).
[17] W. Krech and K. Platov (unpublished).
[18] M. Basler, W. Krech, and K. Y. Platov, Phys. Rev. B **52**, 7504 (1995).
[19] A. K. Jain, K. K. Likharev, J. E. Lukens, and J. E. Sauvageau, Phys. Rep. **109**, 310 (1984).
[20] W. Krech, Ann. Phys. (Leipzig) **39**, 117 (1982).
[21] W. Krech, Ann. Phys. (Leipzig) **39**, 349 (1982).
[22] W. Krech, Ann. Phys (Leipzig) **39**, 50 (1982).
[23] M. Basler, W. Krech, and K. Y. Platov, in *Macroscopic Quantum Phenomena and Coherence in Superconducting Networks*, edited by C. Giovanella and M. Tinkham (World Scientific, Singapore, 1995), pp. 225–234.